AGU PUBLICATIONS

Global Biogeochemical Cycles

RESEARCH ARTICLE
10.1002/2015GB005260

Benthic marine calcifiers coexist with $CaCO_3$-undersaturated seawater worldwide

M. Lebrato[1,2], A. J. Andersson[1], J. B. Ries[3], R. B. Aronson[4], M. D. Lamare[5], W. Koeve[6], A. Oschlies[6], M. D. Iglesias-Rodriguez[7], S. Thatje[8], M. Amsler[9], S. C. Vos[4], D. O. B. Jones[10], H. A. Ruhl[10], A. R. Gates[10], and J. B. McClintock[9]

[1]Scripps Institution of Oceanography, University of California, San Diego, La Jolla, California, USA, [2]Now at Kiel University (CAU), Kiel, Germany, [3]Department of Marine and Environmental Sciences, Marine Science Center, Northeastern University, Boston, Massachusetts, USA, [4]Department of Biological Sciences, Florida Institute of Technology, Melbourne, Florida, USA, [5]Department of Marine Sciences, University of Otago, Dunedin, New Zealand, [6]Biogeochemical Modelling, GEOMAR, Helmholtz Centre for Ocean Research Kiel, Kiel, Germany, [7]Department of Ecology, Evolution and Marine Biology, University of California, Santa Barbara, California, USA, [8]Ocean and Earth Science, University of Southampton, National Oceanography Centre, Southampton, UK, [9]Department of Biology, University of Alabama, Birmingham, Alabama, USA, [10]National Oceanography Centre, University of Southampton Waterfront Campus, Southampton, UK

Key Points:
- At present, 24% of all benthic marine calcifiers experience Mg-calcite undersaturation
- A 50% reduction in $[CO_3^{2-}]$ owing to future OA will cause 57% of all marine benthic calcifiers to experience undersaturation
- To predict responses of calcifying organisms to OA, species-specific mineral compositions must be considered

Supporting Information:
- Supporting Information S1

Correspondence to:
M. Lebrato,
mlebrato13@gmail.com

Citation:
Lebrato, M., et al. (2016), Benthic marine calcifiers coexist with $CaCO_3$-undersaturated seawater worldwide, *Global Biogeochem. Cycles*, *30*, doi:10.1002/2015GB005260.

Received 6 AUG 2015
Accepted 23 MAY 2016
Accepted article online 27 MAY 2016

Abstract Ocean acidification and decreasing seawater saturation state with respect to calcium carbonate ($CaCO_3$) minerals have raised concerns about the consequences to marine organisms that build $CaCO_3$ structures. A large proportion of benthic marine calcifiers incorporate Mg^{2+} into their skeletons (Mg-calcite), which, in general, reduces mineral stability. The relative vulnerability of some marine calcifiers to ocean acidification appears linked to the relative solubility of their shell or skeletal mineralogy, although some organisms have sophisticated mechanisms for constructing and maintaining their $CaCO_3$ structures causing deviation from this dependence. Nevertheless, few studies consider seawater saturation state with respect to the actual Mg-calcite mineralogy ($\Omega_{Mg\text{-}x}$) of a species when evaluating the effect of ocean acidification on that species. Here, a global dataset of skeletal mole % $MgCO_3$ of benthic calcifiers and in situ environmental conditions spanning a depth range of 0 m (subtidal/neritic) to 5600 m (abyssal) was assembled to calculate in situ $\Omega_{Mg\text{-}x}$. This analysis shows that 24% of the studied benthic calcifiers currently experience seawater mineral undersaturation ($\Omega_{Mg\text{-}x} < 1$). As a result of ongoing anthropogenic ocean acidification over the next 200 to 3000 years, the predicted decrease in seawater mineral saturation will expose approximately 57% of all studied benthic calcifying species to seawater undersaturation. These observations reveal a surprisingly high proportion of benthic marine calcifiers exposed to seawater that is undersaturated with respect to their skeletal mineralogy, underscoring the importance of using species-specific seawater mineral saturation states when investigating the impact of CO_2-induced ocean acidification on benthic marine calcification.

1. Introduction

Rising atmospheric pCO_2 and subsequent ocean acidification are expected to result in a decrease in seawater pH, carbonate ion concentration $[CO_3^{2-}]$, and saturation state with respect to calcium carbonate ($CaCO_3$) minerals, which are predicted to have negative effects on marine biomineralization [*Caldeira and Wickett*, 2003; *Doney et al*., 2009]. This could negatively impact marine communities [*Sewell and Hofmann*, 2011] and alter global biogeochemical cycles [*Andersson*, 2014] for which biogenic carbonate mineral production and dissolution are important processes [*Milliman*, 1974; *Opdyke and Wilkinson*, 1993]. Marine biomineralization is the process by which pelagic and benthic organisms actively control and build $CaCO_3$ structures such as shells, tests, spines, and ossicles [e.g., *Lowenstam and Weiner*, 1989]. $CaCO_3$ in marine organisms occurs in various mineral forms or polymorphs, including the following: calcite, aragonite, Mg-calcite, and vaterite. Many benthic calcifiers use amorphous $CaCO_3$ as a transient phase in mineralization, which has radically different properties than its corresponding crystal polymorphs [*Raz et al*., 2000, 2003]. The mineral composition of biogenic $CaCO_3$ is influenced by phylogeny and a number of external factors including temperature, salinity, light, seawater Mg/Ca ratio, seawater carbonate chemistry, life stage, and food supply, which also control growth rate [*Mackenzie et al*., 1983; *Borremans et al*., 2009; *Ries et al*., 2009; *Ries*, 2010].

Despite environmental effects, calcifying organisms exert strong controls on the construction and maintenance of calcareous structures through a wide range of mechanisms, although the extent of control is related

to the organism's specific mode of biomineralization and its energetic status [*Lowenstam and Weiner*, 1989]. For example, many calcifiers have specific ion pumps that aid in creating favorable chemical conditions for $CaCO_3$ deposition (e.g., H^+ pumps and HCO_3^- transporters) [*Zoccola et al*., 2015] and also deposit organic matrices that regulate sites of crystal nucleation and growth [e.g., *Lowenstam and Weiner*, 1989; *Dove et al*., 2003; *Tambutté et al*., 2011]. Recently, it has been proposed that seawater hydrogen ion concentration [H^+] plays a critical role affecting calcifiers ability to construct new $CaCO_3$ [e.g., *Jokiel*, 2011, 2013; *Ries*, 2011a], but it is equally important to consider the susceptibility of marine organisms' specific calcareous minerals to decreasing seawater $CaCO_3$ saturation state. For example, partial skeletal dissolution and/or weaker calcareous structures could render calcifying organisms more vulnerable to predation and/or increase the energetic demands of biomineralization [*Findlay et al*., 2011].

The seawater saturation state with respect to calcareous mineral phases (i.e., Mg-calcite) is defined as follows:

$$\Omega_i = \left\{Mg^{2+}\right\}^x \left\{Ca^{2+}\right\}^{(1-x)} \left\{CO_3^{2-}\right\} / IAP_i, \quad (1)$$

where i is the mineralogy (e.g., calcite, aragonite, and Mg-calcite), x is the skeletal mole fraction of $MgCO_3$ (if present), and IAP_i is the ion activity product at equilibrium with respect to the specific mineral phase [see *Morse et al*., 2006, and references therein]. Ω_i is important because it governs, on the basis of equilibrium thermodynamic principles, whether net formation ($\Omega_i > 1$) or dissolution ($\Omega_i < 1$) of $CaCO_3$ is favored and influences the relative rate at which these reactions proceed.

Many benthic calcite-producing organisms actively incorporate significant amounts of Mg^{2+} into their shells and skeletons during biomineralization (i.e., Mg-calcite). Mg-calcite with greater than 8–12 mol % $MgCO_3$ is more soluble than both pure calcite and aragonite [*Morse et al*., 2006]. Consequently, it has been hypothesized that organisms with Mg-calcite structures exceeding these mole % $MgCO_3$ values could be the most vulnerable to ocean acidification [*Morse et al*., 2006; *Andersson et al*., 2008]. Some experimental results support this hypothesis and show that skeletal mineral solubility impacts calcifiers' relative susceptibility to ocean acidification [*Kuffner et al*., 2008; *Martin and Gattuso*, 2009] while others do not [*Kroeker et al*., 2010; *Thomsen et al*., 2010; *Collard et al*., 2015]. In an experiment that investigated the impact of ocean acidification on 18 species of marine calcifiers spanning a range of $CaCO_3$ polymorphs [*Ries et al*., 2009], five of the six species that exhibited net dissolution under the highest-CO_2 treatment produced a skeleton from the relatively more soluble aragonite and high Mg-calcite polymorphs of $CaCO_3$, rather than from the less soluble low Mg-calcite polymorph. In addition to skeletal mineralogy, important factors that influence the susceptibility of organisms to ocean acidification include the following: the degree to which the organism's biomineral is protected by organic coatings, its ability to regulate pH and carbonate chemistry at the calcification site, its ability to utilize CO_2 via photosynthesis, the shell microstructure, life history, nutritional status, and the physiological condition of the organism [*Kuffner et al*., 2007; *Martin and Gattuso*, 2009; *Ries et al*., 2009; *Holcomb et al*., 2010; *Kroeker et al*., 2010; *Andersson and Mackenzie*, 2011].

Benthic Mg-calcite-secreting organisms, such as echinoderms, coralline algae, and crustaceans, dominate many coastal areas, continental shelves, slopes, and abyssal plains at all depths, and serve important ecosystem and biogeochemical functions, including food supply, ecosystem engineering, carbon storage and export, and elemental cycling [*Lebrato et al*., 2010; *Meadows et al*., 2012; *Andersson*, 2014]. Most studies to date do not consider species-specific seawater mineral saturation state on evaluating organisms' vulnerability to ocean acidification but have interpreted undersaturation with respect to aragonite or calcite as a critical threshold or "tipping point", regardless of organisms' mineral composition [*McNeil and Matear*, 2008; *Steinacher et al*., 2009; *Yamamoto-Kawai et al*., 2009; *Kroeker et al*., 2010; *Comeau et al*., 2013; *Dorey et al*., 2013]. This leads to an incomplete understanding of the influence of seawater carbonate saturation state and the potential consequences of ocean acidification on benthic marine calcifiers and the biogeochemical cycles in which they participate.

In this study, a global dataset of marine $CaCO_3$-producing organisms was collected from the field and from existing literature. Their biomineral compositions were then analyzed (field specimens) or compiled from published studies. Species-specific seawater Ω_i, based upon in situ seawater environmental data, were then calculated for these specimens and then used to model future seawater Ω_i. The objectives of

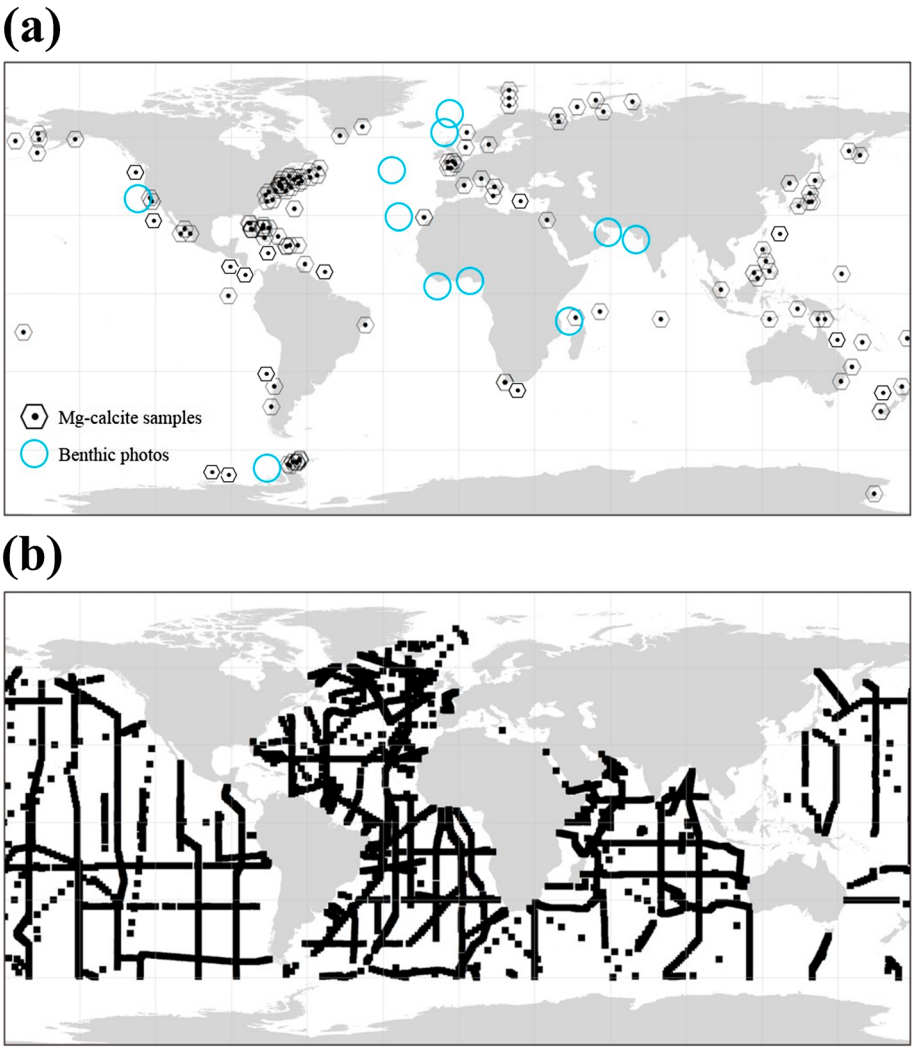

Figure 1. Sample maps. (a) Sample and photo locations. (b) Global coverage of temperature, salinity, and [CO_3^{2-}] data used to obtain the nearest value, in relation to organismal location, for calculating species-specific Ω_i (NEAR 3-D).

the study were to (1) characterize the range of mineralogies of benthic Mg-calcite organisms living in the intertidal/subtidal, neritic zones, continental shelves, slopes, and abyssal plains around the world; (2) determine under what species-specific seawater Ω_i conditions these organisms and mineral phases currently exist; and (3) explore how these conditions could change as a result of future ocean acidification predicted for the next several hundred years. The results of this study have broad implications for the way that seawater saturation state with respect to a particular carbonate mineral phase (Ω_i) is calculated and applied in marine science disciplines and for predicting the impacts of ocean acidification on marine calcifiers.

2. Materials and Methods

The organismal data used in this study were compiled from existing literature at the species level. A large number of echinoderm species were also collected from around the world and analyzed for their Mg content (Figure 1). The best approximation of in situ environmental and carbonate chemistry conditions was retrieved for each sample location based on the GLODAP and WAVES databases [*Key et al*., 2004]. Details on literature mining, data classification, data analysis, and modeling are provided below. Detailed calculations and technical considerations involved in the calculation of seawater saturation state and solubilities for Mg-calcite (Tables S1 and S2 and Figures S1–S5 in the supporting information), additional information about the distribution of organismal and environmental samples (Tables S1 and S2 and Figures 1 and S2), the numerical

modeling of the [CO_3^{2-}] reduction scenarios (Figure S4), and the master dataset (Tables S1–S4) are provided in the Supporting Information (SI).

2.1. Literature-Based Mg-Calcite Data

All measurements of mole % $MgCO_3$ of the investigated taxa and species (with the exception of the echinoderms, which were analyzed as part of the present study) were mined from the existing literature to generate the most comprehensive and taxonomically broad Mg-calcite dataset presently available (Figure 1 and Tables S1–S3). Most of the literature-based mole % $MgCO_3$ data were determined by powder X-ray diffraction and/or single collector inductively coupled plasma–mass spectrometry (ICP-MS) (Tables S2–4). The selection criteria for data derived from the literature was that (i) the organism was identifiable at the species level, (ii) weight % (wt %) or mole % $MgCO_3$ were measured, and (iii) reliable geographic and depth information were provided to link the species mole % $MgCO_3$ with the seawater conditions for each sample location. These data permitted calculation of species-specific seawater mineral saturation states. The following taxa, identified at the species level were assessed in the present study (see Tables S1–S4 for additional taxonomic and identifying information): Echinodermata—Asteroidea (49 species), Echinoidea (34 species), Ophiuroidea (23 species), and Crinoidea (21 species); Rhodophyta—Corallinaceae (26 species); benthic Foraminifera (12 species); Anthozoa—Hydrocorallia (3 species), Hexacorallia (12), and Octocorallia (35 species); Bryozoa (10 species); Brachiopoda (8 species); Mollusca—Amphineura (1 species), Bivalvia (7 species), Cephalopoda (3 species), Gastropoda (6 species), and Scaphopoda (1 species); and Crustacea—Cirripedia (5 species), Amphipoda (1 species), Decapoda (8 species), Stomatopoda (1 species), and Isopoda (1 species).

2.2. Skeletal Mg-Calcite Measurements

Skeletal mole % $MgCO_3$ data for the echinoderms were obtained through ICP-MS analysis of field-collected samples (Figure 1 and Tables S1–S4). Adult echinoderms were collected between years 2008 and 2011 from 2 to 1300 m depth in the Atlantic, Pacific, Arctic, and Southern Oceans (methods detailed in *Lebrato et al*. [2010] and *McClintock et al*. [2011]) (Tables S1 and S3). Note that these new analyses are unrelated to *Lebrato et al*. [2010], where "whole bodies" were measured to determine total carbon content. Here only skeletal material without associated organic material was analyzed. Samples were stored at −20°C in ziplock bags, freeze-dried for 48 h, and finally ground to powder. Percent $MgCO_3$ was measured with a Varian 820 inductively coupled plasma–mass spectrometer (ICP-MS) at the University of North Carolina at Chapel Hill (USA). A 0.5 g sample of pulverized material was digested for 2 h in *Aqua Regia* at 90°C. Duplicate samples were run every 15 samples, and in-house secondary standards were run every 33 samples. Certified standards and blanks were run every 68 samples. Antarctic samples were analyzed at Actlabs in Ancaster, Ontario, Canada (methods described in *McClintock et al*. [2011]). In brief, frozen samples were thawed and dissected and then soaked in 10% NaClO to remove organic matter. The remaining carbonate was vacuumed onto filter paper, rinsed with Milli-Q water, and then dried at 50°C for 48 h. Percent $MgCO_3$ was obtained using a PerkinElmer inductively coupled plasma (ICP) atomic emission spectrometer. The samples were divided in 90 to 500 mg splits and dissolved in nitric acid (HNO_3) and hydrochloric acid (HCl) in a molar ratio of 1:3 for 2 h at 95°C. Several U.S. Geological Survey standards were analyzed every 13 samples. Quality control results of the ICP-MS work are summarized in Table S4.

2.3. Linking Mg-Calcite Measurements to In Situ Physical and Chemical Data

Each organismal sample and their corresponding mole % $MgCO_3$ (either mined from the literature or measured directly) was associated with a latitude, longitude, and depth, allowing compilation of approximate in situ temperature, salinity, and carbonate chemistry data for each specimen (Table S2 and Figures 1 and S2). These environmental properties were extracted to the nearest value in a 3-D matrix in the GLODAP dataset [*Key et al*., 2004] using gridded station data from GLODAP/WAVES (http://cdiac3.ornl.gov/waves/discrete/) at a global scale. A regional dataset in the North Atlantic Ocean [*Dumousseaud et al*., 2010] was used to study temporal changes in Mg-content of calcite and Ω_i (Figure S5; see SI for details on how [CO_3^{2-}] was calculated). These databases were used because they contain the most complete and accurate seawater carbonate chemistry data currently available for the purpose of the present study.

It is important to note that the field data may not represent the exact in situ conditions experienced by the organisms and do not account for variability owing to oceanographic and seasonal processes. The calculations represent temporal "snapshots", with the actual species-specific seawater $\Omega_{Mg\text{-}x}$ varying throughout

the year following environmental parameters that are discussed below (e.g., Figure 2). However, the variability in physical and chemical conditions at the depths considered here (seafloor) is substantially smaller than that experienced in the surface mixed layer. Also, the amplitude of seasonal variation is dampened as a function of decreasing latitude and increasing water depth.

ArcGIS 10.0 [*Environmental Systems Research Institute*, 2011] and the 3-D analytical tool "NEAR 3-D analysis" were used to link environmental seawater conditions with the organisms' parameters and mole % $MgCO_3$. This approach permitted evaluation of the diagonal distance between each organismal input parameter (latitude, longitude, and depth) and the nearest seawater datum (temperature (T), salinity (S), and [CO_3^{2-}]) at a specific latitude, longitude, and depth. The the prerequisite for data adoption was a matching data set XYZ (including organismal parameter) versus $X_iY_iZ_i$ (including ambient seawater property). Both data sets were plotted on a 2-D field and merged into a single 3-D field, and then the nearest seawater datum to the specimen was determined using a diagonal line in a 3-D matrix (Table S2). Additionally, each datum was individually checked to verify that the NEAR 3-D approach worked correctly. When the prediction was not sufficiently accurate, the closest value was manually selected. This procedure ensured selection of the most relevant seawater parameters for a given biological specimen.

2.4. Seawater Ω_i Calculations

Seawater saturation state with respect to calcite, aragonite, and calcite of a given mole % $MgCO_3$ ($\Omega_{Mg\text{-}x}$) was calculated according to equation (1). Detailed calculations, equations, constants, and corrections for temperature, salinity, and hydrostatic pressure used for calculations of seawater Ω_i with respect to all carbonate mineralogies in this study are available in the SI. Corrections for the influence of temperature and pressure on solubility were made in a manner similar to the correction of calcite solubility. This allows detailed seawater Ω_i approximations calcite of any Mg-content, thus going beyond the standard surface ocean conditions (e.g., total alkalinity, dissolved inorganic carbon, pH, temperature of 25 °C, salinity of 35) that are typically considered in calculating seawater Ω_i for calcareous organisms [*Morse et al*., 2006; *Andersson et al*., 2008; *Lavigne et al*., 2011, Seacarb software]. This approach represents a new method to approximate seawater Ω_i for Mg-calcite bearing organisms at any temperature, salinity, and pressure (depth). The corresponding equations are provided in an *Excel* spreadsheet, available from the corresponding author upon request.

Individual ion activity products (IAP_i) employed in the $\Omega_{Mg\text{-}x}$ calculations were based on the biogenic "clean" and biogenic "minimally prepared" experimental solubility curves (Figure S1) [*Plummer and Mackenzie*, 1974; *Bischoff et al*., 1987]. The two curves differ in the way that the experimental materials were prepared. Although there is currently insufficient information to determine which experimental solubility curve best represents the solubility of Mg-calcite mineral phases in the natural environment, several studies support the use of the minimally prepared solubility curve because it appears more compatible with complementary field and experimental results [*Tribble et al*., 1995; *Andersson et al*., 2007]. Therefore, results are presented that employ both solubility curves, with discussion focused on results derived using the minimally prepared solubility curves (Figure S1).

2.5. Photographic Evidence for Calcifying Organisms Inhabiting Undersaturated Seawater

As a complement to the quantitative aspect of this study, photographs of benthic Mg-calcite organisms at shelf, slope, rise, and abyssal depths in the Atlantic, Pacific, Indian, and Southern Oceans were obtained and analyzed to verify that Mg-calcite organisms live in waters from 0 to 5600 m and at $\Omega_{Mg\text{-}x}$ values near or below 1 (Table S5). The photographs were obtained using video cameras mounted on remotely operated or autonomous underwater vehicles, towed cameras, sled cameras, and still cameras [*Lebrato and Jones*, 2009; *Eastman et al*., 2013] (Table S5).

Each photograph was associated with a location (latitude, longitude, and depth) and environmental data (T, S) obtained during the corresponding expedition (Table S5). If in situ T and S data were not available, data were compiled along with in situ [CO_3^{2-}] using the previously described ArcGIS NEAR 3-D analysis technique (including the manual check). Values of $\Omega_{Mg\text{-}x}$ were calculated for each organism at each location based on mean skeletal mole % $MgCO_3$ for the same species (when available), a similar species in the same class, or for the geographically closest species available (according to latitude and depth; see Table S5 for assumptions and data used). Although these qualitative data should be interpreted with caution, as organismal mineralogy is complex and highly variable, this approach yields insight into the distribution of $\Omega_{Mg\text{-}x}$ for benthic marine calcifiers in the deep-sea (2000 to 5600 m). It should also be noted that the photos presented in Figure 6

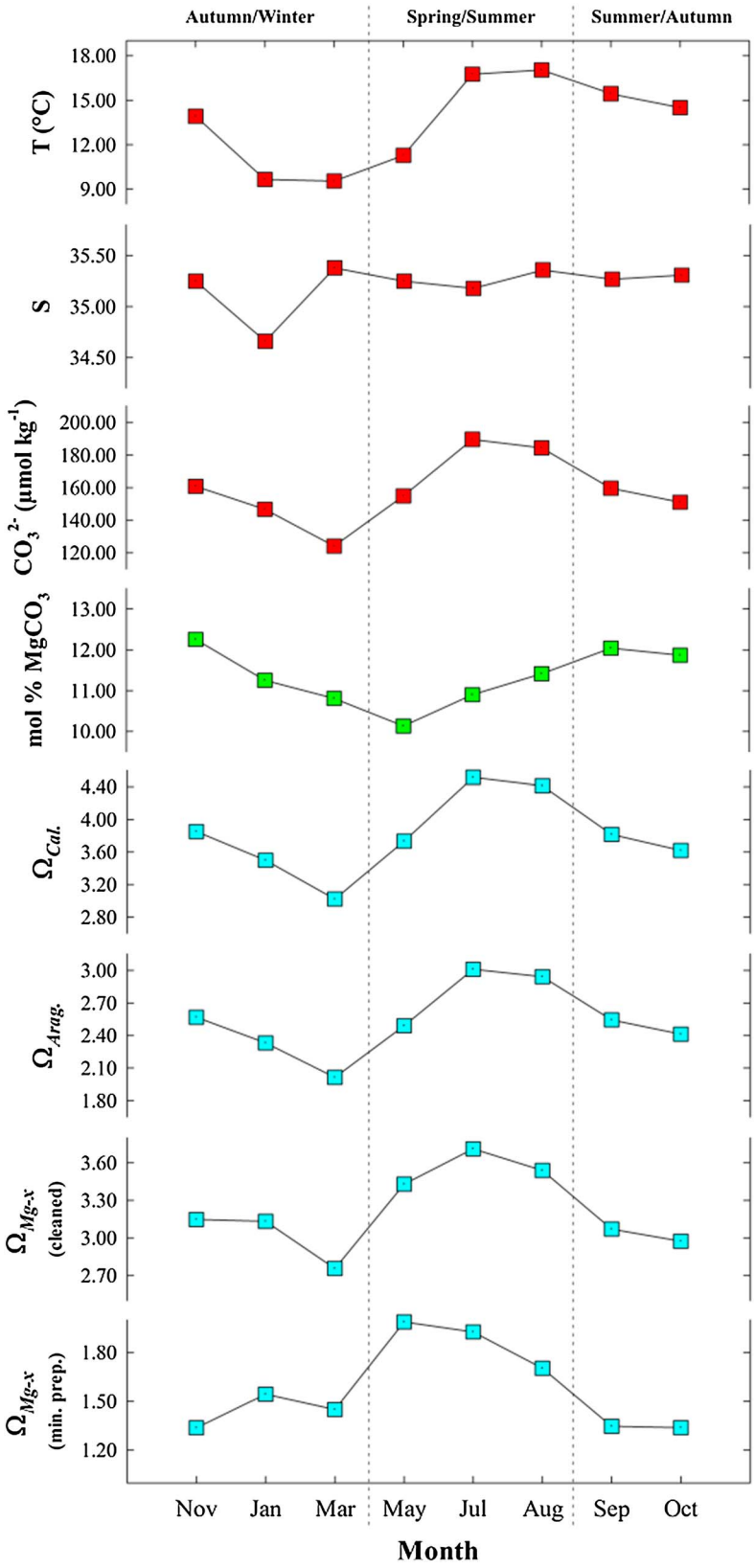

Figure 2. Seasonal changes in the skeletal mole % $MgCO_3$ in the coralline alga *Corallina squamata*. The coralline Mg-calcite samples were obtained over 11 months at 5 m on the Dorset coast (UK, Atlantic Ocean) [*Haas et al.*, 1935]. Calculated seawater Ω_i is plotted over time, with seasonal variations in skeletal mole % $MgCO_3$ driven by seasonal variability in seawater temperature.

represent only a small subset of all images used in this analysis. However, all sampling locations for which photographs were obtained are plotted in Figure 6, with corresponding data provided in Table S5.

2.6. Modeling of [CO_3^{2-}] Decrease to Predict Future Ω_i

In order to better understand how oceanic Ω_i will change in the future in response to increasing pCO_2 and temperature, [CO_3^{2-}] was calculated for surface and bottom waters at future time points using the UVic Earth System Model [*Keller et al*., 2012] (Figure S4). CO_2 emissions were forced with the Representative Concentration Pathway 8.5 scenario, which is a "business-as-usual", high-CO_2-emission scenario [*Keller et al*., 2014]. Decreases in [CO_3^{2-}] of 20 and 50% from modern values were used to estimate the timing of these scenarios for the surface and seafloor (−20% sfc: 2050–2065; −20% sfl: 2150–2700; −50% sfc: 2090–2120; −50% sfl: 2500–3000+; white areas in the figure maps are beyond year 3000; Figure S4). The output represents the globally averaged change in [CO_3^{2-}] over time for surface and bottom waters. The years provide an approximation of this change because [CO_3^{2-}] in deeper water masses decline at a slower rate than in surface waters (see Figures 4 and S4). The model projections include the impact of anthropogenic CO_2 invasion as well as the effect of increasing ocean temperature on this process.

3. Results

3.1. Percent $MgCO_3$ of organisms' Mg-Calcite

The Mg content of the organisms in the global dataset ranged from <1 to >27 mole % $MgCO_3$, varying significantly among and within phyla, classes, and species (Figure 3a). The lowest mean mole % $MgCO_3$ content was observed in the class Anthozoa (Hydrocorallia and Hexacorallia) and phylum Mollusca (Bivalvia, Amphineura, Scapopoda, and Gastropoda) with a mean [±SD (standard deviation)] of 1.96 ± 3.80 and 1.27 ± 1.33 mol % $MgCO_3$, respectively. The highest mole % $MgCO_3$ was observed in the Rhodophyta (coralline algae, mainly Corallinaceae) with a mean (±SD) of 16.29 ± 5.02 mol % $MgCO_3$, but this phylum also showed the greatest range from 7.11 to 27.27 mol % $MgCO_3$. Large variability was also observed within Echinodermata (Classes Asteroidea, Echinodea, Ophiuroidea, and Crinoidea), Protista (Foraminifera), Anthozoa (Octocorallia), Bryozoa, Mollusca (Cephalopda), and Crustacea (Decapoda), ranging from 0.40 to 18.14 mol % $MgCO_3$ (Figure 3a).

In general, the Mg content of organisms with greater than 5 mol % $MgCO_3$ followed an inverse parabolic distribution as a function of latitude, with decreasing Mg content toward the poles (Figure 3b). In contrast, organisms with less than 5 mol % $MgCO_3$ showed no apparent trend as a function of latitude. Considering Mg content as a function of depth, large variability was observed between 0 and 200 m (0.19 to 27.26 mol % $MgCO_3$), there were almost no occurrences of organisms with greater than 16 mol % $MgCO_3$ between 100 and 200 m, and there were no organisms with greater than 9 mol % $MgCO_3$ below 600 m (Figure 3c). Organisms containing less than 5 mol % $MgCO_3$ were mainly observed between 0 and 100 m, with a few observations at 700 m. The rare occurrence of organisms with <5 mol % $MgCO_3$, compared to organisms with a higher Mg content, at depths greater than 100 m is puzzling and raises questions about whether this reflects a true biological pattern or is simply a sampling artifact. Similarly, measurements of mole % $MgCO_3$ of organisms collected from depths greater than 1000 m were uncommon in the literature (only seven samples from 1000 to 4000 m, excluding the photo analysis), although there is ample evidence that Mg-calcite-producing organisms exist at these depths [*Sokolova*, 1972; *Gage and Tyler*, 1991].

3.2. Species-Specific Seawater Ω_i Under Present Conditions in Benthic Habitats

Seawater saturation states with respect to calcite ($\Omega_{Cal.}$) and aragonite ($\Omega_{Arag.}$) exhibited an inverse parabolic relationship from pole-to-pole at all depths (i.e., lower seawater saturation at high latitudes), with $\Omega_{Cal.}$ ranging from 1.1 to 7.7 and $\Omega_{Arag.}$ ranging from 0.7 to 5.1 from high to low latitudes (Figure 4; 0.3% to 1.5% of locations were less than 1 with respect to $\Omega_{Cal.}$ and $\Omega_{Arag.}$, respectively). In general, the location-specific seawater $\Omega_{Cal.}$ and $\Omega_{Arag.}$ decreased with depth, a trend driven by decreasing [CO_3^{2-}] related to increasing respiratory CO_2 in the water masses, and increasing solubility owing to increasing pressure and decreasing temperature (Figure 5). In contrast, at depths <200 m, seawater $\Omega_{Cal.}$ and $\Omega_{Arag.}$ ranged from 2.1 to 7.7 and from 1.4 to 5.1, respectively, with the broad range resulting from the large temperature variation (−0.86 to 39.38°C) as a function of latitude (Table S1 and Figure 5). For depths greater than 1000 m, seawater $\Omega_{Cal.}$ and $\Omega_{Arag.}$ were always below 2 (except in one case), with most values very near or below 1 (Figures 5 and 6).

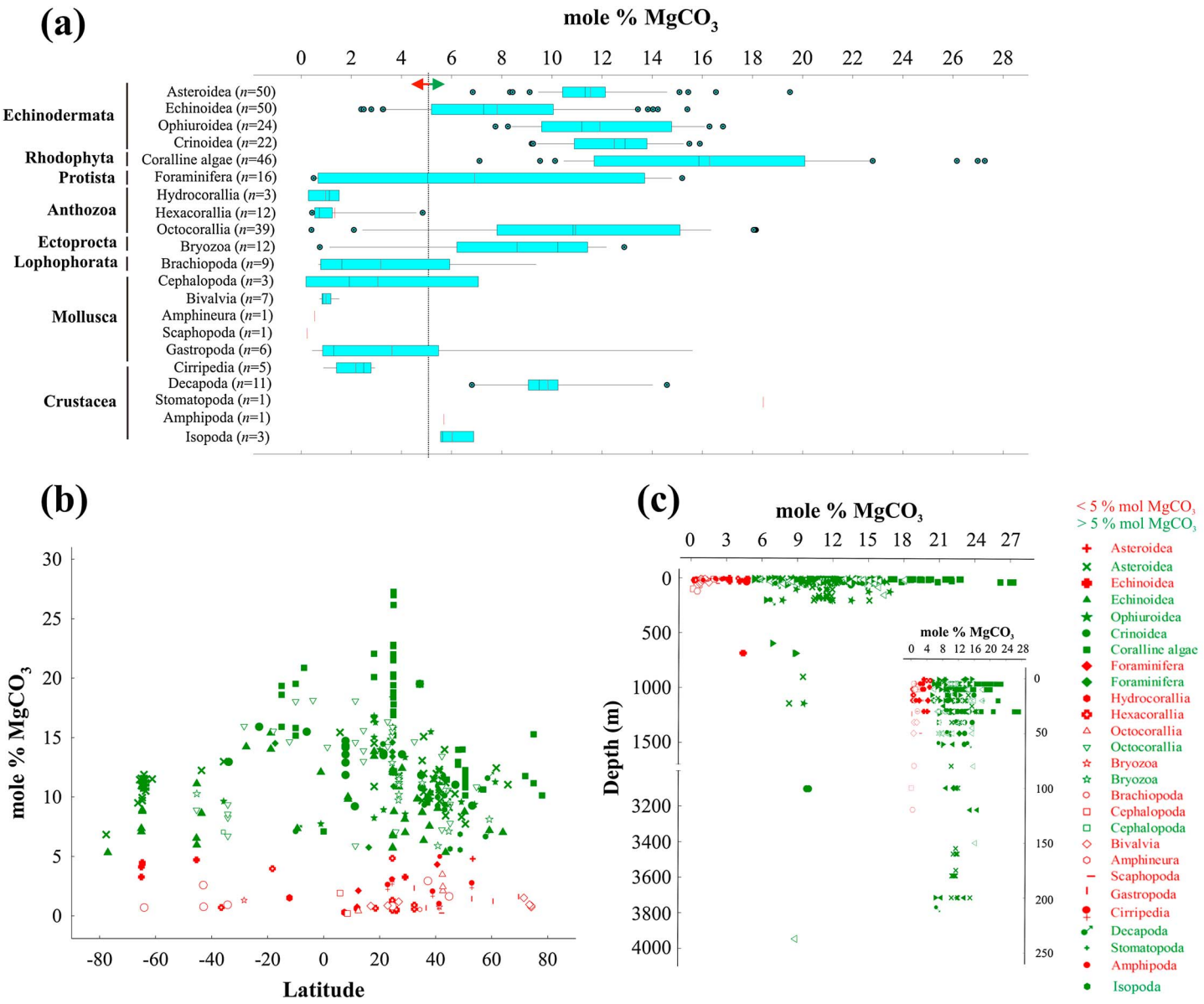

Figure 3. Patterns of Mg-calcite skeletal mineralogy. (a) Box plots of skeletal mole % $MgCO_3$ of all taxa investigated in this study (n = sample size for each taxon), including minimum and maximum values (box edges), outliers (circles), and the mean value (red line inside the boxes). The vertical black dotted line in Figure 3a represents 5 mol % $MgCO_3$ (Figure 3b; red = <5 mol % $MgCO_3$; green = >5 mol % $MgCO_3$). Also included are trends of skeletal mole % $MgCO_3$ by (b) latitude and (c) depth. See Tables S1–S3 for additional information about skeletal/shell mineralogy.

If one were to consider seawater $\Omega_{Mg\text{-}x}$ for any specific Mg-calcite phase (e.g., 15 mole % $MgCO_3$), the shape of the $\Omega_{Mg\text{-}x}$ latitudinal trend would be similar to trends observed for aragonite and calcite (Figures S3d and S3e). Considering the species-specific seawater $\Omega_{Mg\text{-}x}$ for these samples, however, there were no obvious latitudinal trends due to the differing mineralogies (solubilities), temperatures, and depths (pressure and $[CO_3^{2-}]$ effects; Figures 3–5, Table S1, and Figures S2 and S3). For Mg-calcite containing < 5 mole % $MgCO_3$, the species-specific $\Omega_{Mg\text{-}x}$ ranged from 2.1 to 6.8 at depths less than 1000 m, with no obvious trend toward higher latitudes. For Mg-calcite containing > 5 mol % $MgCO_3$, the species-specific $\Omega_{Mg\text{-}x}$ ranged from 0.3 to 5.8 at depths less than 1000 m. A total of 24.1% of the species were exposed to seawater $\Omega_{Mg\text{-}x} < 1$ across all studied latitudes and depths. Although there was no clear trend of seawater $\Omega_{Mg\text{-}x}$ with latitude, a greater proportion of the low-latitude species were found inhabiting undersaturated conditions (22.1% were exposed to seawater $\Omega_{Mg\text{-}x} < 1$; Figures 4 and 5 bottom panels) when compared with the

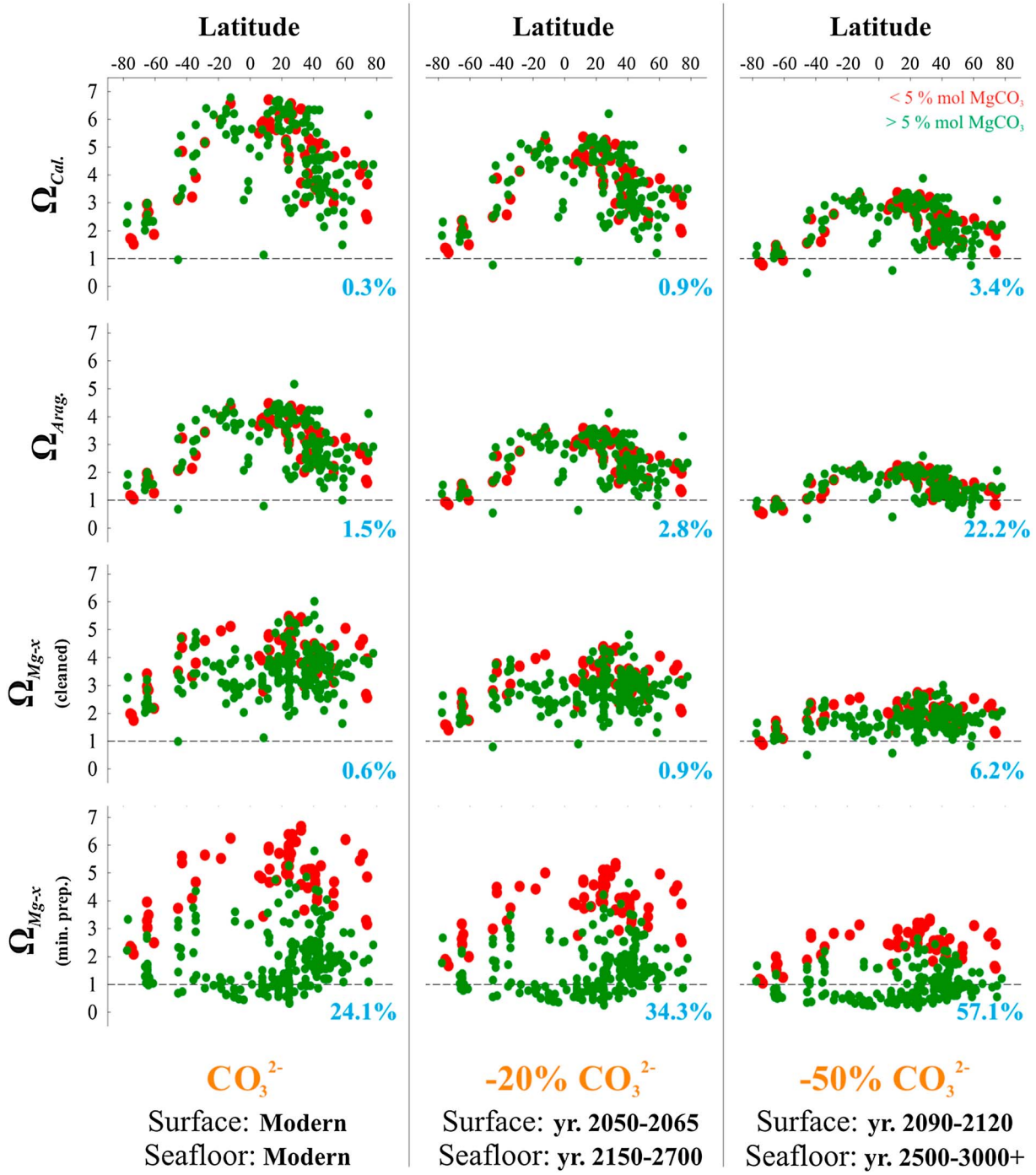

Figure 4. Calcite, aragonite, and taxon-specific seawater-Ω_i patterns versus latitude. Seawater-Ω_i is calculated using the organisms' skeletal mole % $MgCO_3$ and their in situ seawater conditions in the modern and future ocean, with $[CO_3^{2-}]$ reduced by 20% in years 2050–2065 (surface) and 2150–2700 (seafloor), and by 50% in years 2090–2120 (surface) and 2500–3000+ (seafloor). The dotted lines represent equilibrium Ω_i (i.e., $\Omega_i = 1$), below which mineral dissolution theoretically begins pursuant to the principals of equilibrium thermodynamics. The percentages of taxa living in undersaturated conditions with respect to their species-specific mineralogies (i.e., $\Omega_i < 1$) are shown in blue.

high-latitude species (2%). The highest proportion of species exposed to undersaturation was observed at depths <2000 m, and especially at depths <200 m in the coastal zones (Figure 4). Seawater undersaturation for most species appears to extend from depths of 2000 to 5600 m (90% of the taxa at these depths; Figures 3 and 4). The range of values for species-specific seawater $\Omega_{Mg\text{-}x}$ decreased as a function of depth.

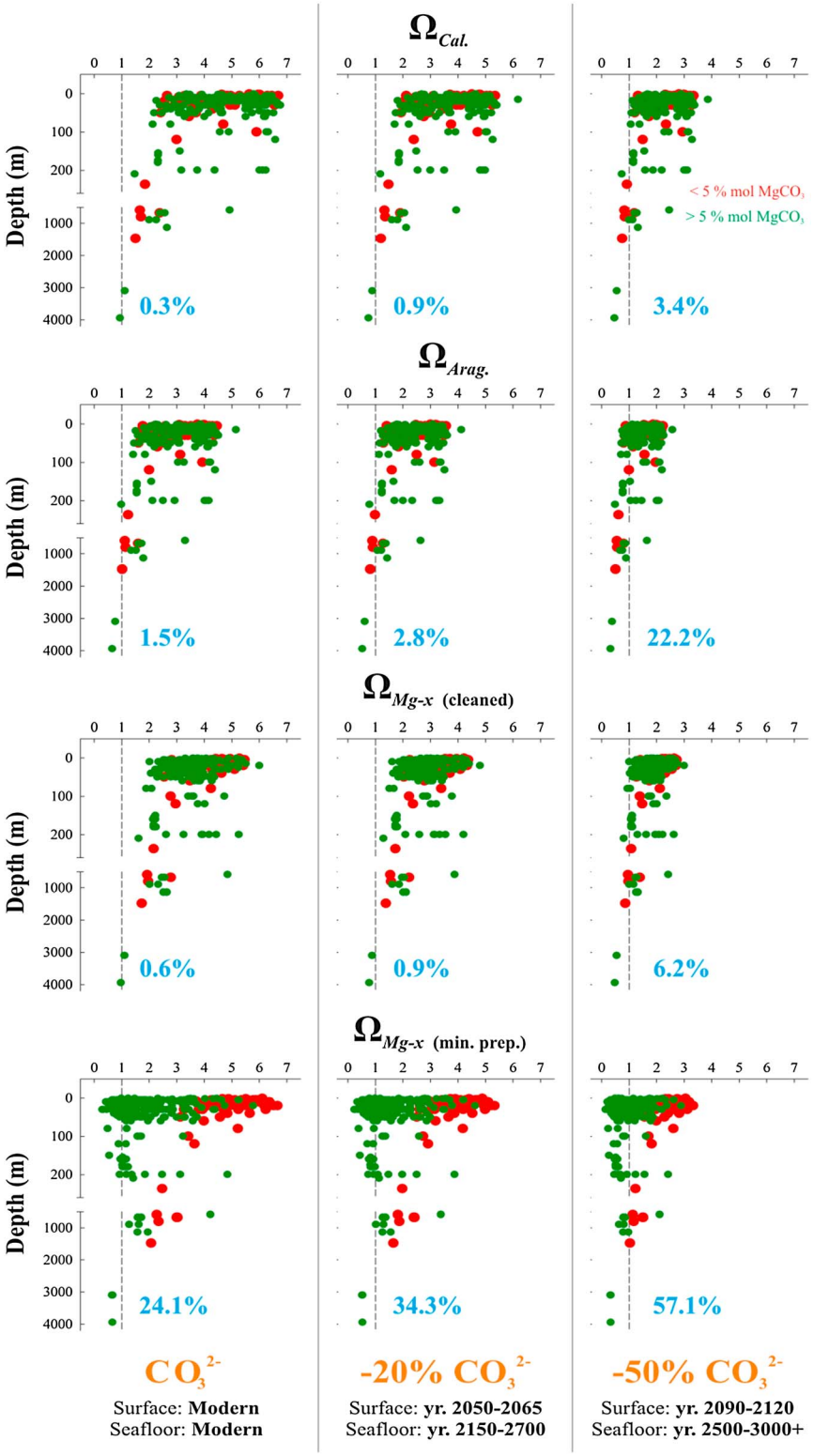

Figure 5. Taxon-specific seawater-Ω_i patterns versus depth. Seawater-Ω_i is calculated using the organisms' ambient seawater conditions and the skeletal mole % $MgCO_3$ in the modern and future ocean, with [CO_3^{2-}] reduced by 20% in years 2050–2065 (surface) and 2150–2700 (seafloor), and by 50% in years 2090–2120 (surface) and 2500–3000+ (seafloor). The dotted lines represent equilibrium Ω_i (i.e., $\Omega_i = 1$), below which mineral dissolution theoretically begins pursuant to the principals of equilibrium thermodynamics. The percentages of taxa living in undersaturated conditions with respect to their species-specific mineralogies (i.e., $\Omega_i < 1$) are shown in blue.

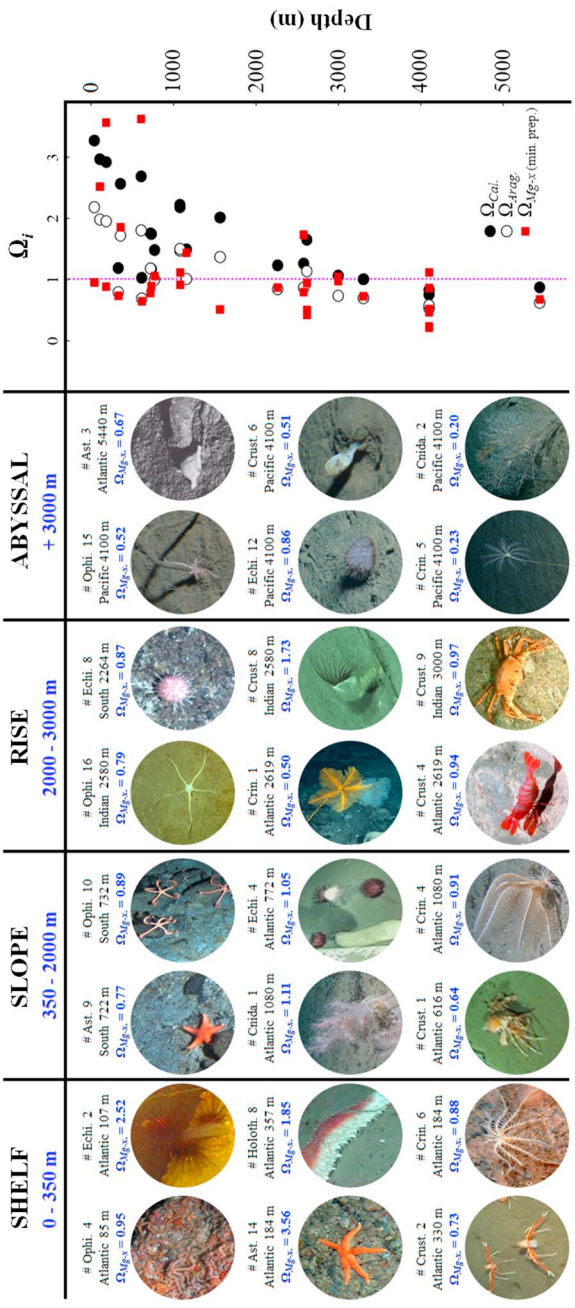

Figure 6. Calcareous organisms at shelf, slope, rise, and abyssal plain (Ophi: Ophiuroidea, Echi: Echinoidea, Ast: Asteroidea, Holoth: Holothuroidea, Cnida: Cnidaria, Crin: Crinoidea, Crust: Crustacea; see Table S5 for all species). Composite photographs from the Atlantic, Pacific, Indian, and Southern Oceans from 0 to 5600 m depth in the modern ocean (complete results in Table S5). In situ $\Omega_{Mg\text{-}x}$ was calculated using Mg content of the specimen imaged in the photograph. For photos lacking physical specimens, in situ $\Omega_{Mg\text{-}x}$ was calculated using mean Mg content of other individuals of the same species (when available), of the closest available species (according to latitude and depth), or of other species within the same class. In situ seawater parameters were obtained from a NEAR 3-D analysis (see section 2). Ambient seawater conditions along with calculated seawater pH_{total} and CO_2 are presented in Table S5. The plot on the right side shows the calculated seawater Ω_i profiles for all specimens (calcite, aragonite, and Mg-calcite) with depth, revealing that most higher Mg-calcite-producing organisms are inhabiting seawater that is undersaturated with respect to their shell mineralogy across all four facies (shelf, slope, rise, abyssal plain). Pink dotted line represents equilibrium Ω_i (i.e., $\Omega_i = 1$), below which mineral dissolution theoretically begins pursuant to the principals of equilibrium thermodynamics. Data represent modern ocean conditions.

3.3. Species-Specific Seawater Saturation States Under Future Conditions in Benthic Habitats

To project species-specific $\Omega_{Mg\text{-}x}$ into the future, two scenarios anticipated for years 2050–2065 (surface)/2150–2700 (seafloor) and 2090–2120 (surface)/2500–3000+ (seafloor) were assessed. In these scenarios, the general trends of seawater Ω_i with respect to calcite, aragonite, and Mg-calcite, remained the same as a function of latitude and depth compared with the present-day ocean, but at lower saturation states (Figures 4 and 5). In response to a 20% decrease in [CO_3^{2-}], almost all locations were supersaturated with respect to calcite, 2.8% were undersaturated with respect to aragonite, and 34.3% were undersaturated with respect to species-specific $\Omega_{Mg\text{-}x}$ across all studied latitudes and depths. A 50% reduction in [CO_3^{2-}] resulted in seawater undersaturation at 3.4% of locations for calcite, 22.2% for aragonite, and 57.1% for species-specific $\Omega_{Mg\text{-}x}$ across all studied latitudes and depths, with seawater undersaturation for all species between 2000 and 5600 m depth.

4. Discussion

At present, a surprisingly high proportion of benthic marine calcifying species (24.1% across all studied latitudes and depths, and 90% below 2000 m; Figures 5 and 6) are inhabiting seawater that is undersaturated with respect to their species-specific mineralogy, especially at low latitudes (equatorial). These taxa are primarily coralline algae, crinoids, and octocorals, with Mg content that is typically greater than 14 mol % $MgCO_3$, (Figure 4, bottom panels). High (polar) latitude oceans, in contrast, contain a lower proportion of species living in seawater undersaturated with respect to their species-specific mineralogies because their overall mole % $MgCO_3$ is lower than at tropical latitudes, although many appear to exist close to a metastable equilibrium with seawater (i.e., $\Omega_{Mg\text{-}x} = 1$). Given the relatively stable conditions in seawater carbonate chemistry experienced for hundreds of thousands of years prior to the Industrial Revolution [*Zeebe*, 2012], it appears that many organisms have been living at or below equilibrium ($\Omega_{Mg\text{-}x} \leq 1$) for an extended time. It can therefore be assumed that marine benthic calcifiers have long possessed physiological adaptations that allow them to build and maintain calcareous structured under such low $\Omega_{Mg\text{-}x}$ conditions. Other environmental properties (e.g., food availability) may also help or hinder organisms' ability to overcome negative effects of low seawater $\Omega_{Mg\text{-}x}$ in these environments.

Yet, the question remains as to how marine benthic calcifiers inhabiting seawater of $\Omega_{Mg\text{-}x} < 1$ maintain and build their calcareous structures, which based upon thermodynamic principles, should dissolve. Many benthic species have calcareous skeletons and/or shells that are covered with tissue and/or organic compounds while the organisms are alive (e.g., periostraca, epicuticles, and epiderma) that isolate and separate the Mg-calcite from seawater to protect the structures from dissolution [*Ries et al*., 2009]. The protective value of organic coatings is apparent after the organism dies, as unprotected shells and skeletons tend to dissolve rapidly [*McClintock et al*., 2009] and often do not become part of the sedimentary record in most modern marine environments (excluding carbonate platforms and coral reef environments). This is pronounced in polar waters and the deep sea, where seawater tends to be highly corrosive to carbonate minerals [*Waldbusser et al*., 2011; *Walker et al*., 2013]. Organisms that have access to a regular and adequate supply of energy via heterotrophy and/or photosynthesis are also more likely to overcome constraints imposed by low seawater $\Omega_{Mg\text{-}x}$ [*Sokolova*, 1972; *Holcomb et al*., 2010; *Smith et al*., 2013; *Castillo et al*., 2014]. For example, mollusks in the Kiel Fjord (Baltic Sea) thrive and spawn under chemically unfavorable conditions (very high CO_2) because these conditions coincide with a large, seasonal food supply connected to regional upwelling [*Thomsen et al*., 2010]. Similarly, the high energy available at low latitudes, due to higher irradiance and, thus, higher rates of photosynthesis, probably explain why many coralline algae with high Mg-calcite content (14 to 27 mol % $MgCO_3$) are able to thrive despite species-specific seawater undersaturation (Figures 3 and 4). Furthermore, organisms living in low $\Omega_{Mg\text{-}x}$ conditions may be able to reallocate energy to maintain calcification, but at the expense of other functions, such as growth, energy storage, and reproduction [*Wood et al*., 2008; *McCulloch et al*., 2012; *Dupont et al*., 2013]. Observations also suggest that deep-sea and some polar Mg-calcite organisms tend to have softer body structures and thinner skeletons than elsewhere, but it is unknown whether this is a consequence of hydrostatic pressure, low temperature, seawater carbonate chemistry, low predation, or any other factor or combination of factors [*Gage and Tyler*, 1991; *Aronson et al*., 2007; *Watson et al*., 2012] (Figure 6).

The observation that many marine calcifiers inhabit depths that are undersaturated with respect to their species-specific mineralogies (Figure 6 and Table S5) suggests that they are utilizing compensatory physiological mechanisms to cope with undersaturated conditions. The Mg content of shallow water coralline algal calcite varies on monthly timescales by up to 2 mol % (Figure 2) [*Haas et al*., 1935]. This translates to shifts in seawater $\Omega_{Mg\text{-}x}$ from 1.20 in November to 1.90 in February of the same year (and back to 1.20 in October) in coastal waters of the UK, corresponding to a greater than 50% change (Figure 2). Although these annual changes in Mg content should confer additional resilience during colder months of the year, it is presently unclear whether this is an active survival strategy or a passive thermodynamic or kinetic response to fluctuations in seawater temperature and $[CO_3^{2-}]$.

Thermodynamic principles suggest that marine organisms require more energy to biocalcify under more acidic conditions. Thus, organisms' specific responses to ocean acidification should be dictated by their energy budgets and whether there are thresholds beyond which they cannot divert additional energy from other physiological functions without negative consequences to their overall fitness [*Dupont et al*., 2013]. It has also been shown that some marine calcifiers, such as whelks and coralline red algae, deposit increasingly stable mineral phases (decrease in Mg content) in response to ocean acidification (see also Figure 2 for temporal changes), while others (e.g., calcareous serpulid worms) deposit increasingly less stable mineral phases in response to ocean acidification, and still others (e.g., urchins, lobsters, crabs, and shrimp) show no mineralogical response to ocean acidification [*Ries*, 2011b].

As seawater $\Omega_{Mg\text{-}x}$ changes in benthic ecosystems as a function of depth and latitude, some organisms may adapt to ocean acidification by progressively migrating to nearby regions of higher seawater saturation state. For example, it was observed that 95% of all deep-sea corals live at depths above the aragonite saturation horizon [*Guinotte et al*., 2006]. Nonetheless, it is likely that some taxa will not be able to tolerate decreasing saturation states and could suffer significant mortality and population declines, as did certain benthic foraminifera during the Paleocene-Eocene Thermal Maximum ocean acidification event [*Hönisch et al*., 2012; *Clarkson et al*., 2015]. Calcareous organisms with <5 mol % $MgCO_3$ from the present dataset that inhabit depths shallower than 4000 m will remain in supersaturated seawater conditions even after a 50% decline in seawater $[CO_3^{2-}]$ (Figures 4 and 5), potentially providing them with a competitive advantage over calcifiers with a higher mole % $MgCO_3$. Note though that seawater chemistry varies between the ocean basins and, in general, seawater $\Omega_i = 1$ occurs at a much shallower depth in the Pacific Ocean compared to the Indian and Atlantic Oceans [*Andersson*, 2014]. The present study shows that many shallow-water Mg-calcite organisms, and most deep-sea Mg-calcite organisms inhabiting waters deeper than 2000 m, already inhabit undersaturated seawater, suggesting that they have evolved the biological and physiological mechanisms needed to survive in seawater $\Omega_{Mg\text{-}x} \leq 1$. It should be emphasized, however, that it remains unknown how such deep-sea calcifiers will respond to the rapid declines in seawater $\Omega_{Mg\text{-}x}$ accompanying anthropogenic ocean acidification, as these organisms generally originated in environments when seawater saturation state was relatively stable, albeit low [*Gage and Tyler*, 1991].

To accurately predict the impacts of ocean acidification on benthic marine taxa and ecosystems, it is critical to determine whether there are thresholds or so-called tipping points (or points-of-no-return) in organisms' responses [*Hall-Spencer et al*., 2008]. Some studies have suggested $\Omega_{Arag.} = 1$ as a tipping point, but this value is not theoretically appropriate for taxa with skeletons that are more (or less) soluble than aragonite [*Feely et al*., 2004; *Hall-Spencer et al*., 2008; *McNeil and Matear*, 2008; *Steinacher et al*., 2009; *Yamamoto-Kawai et al*., 2009; *Kroeker et al*., 2010] (Figures 4–6 and S1 and S3). This study highlights the need to consider species-specific $\Omega_{Mg\text{-}x}$ in assessing tipping points in biological responses to ocean acidification.

Our ability to predict calcareous organisms' responses to ocean acidification is hindered by a poor understanding of the physiological controls on Mg incorporation into calcareous structures, especially in relation to changes in seawater $[CO_3^{2-}]$. We also have limited knowledge of the role that Mg incorporation plays in the formation and stabilization of amorphous calcium carbonate, which appears to be a transient phase in some modes of biological mineralization, and how this mineral phase is impacted by changes in seawater carbonate chemistry [*Raz et al*., 2000, 2003]. Experiments and field observations have indicated that Mg content in some taxa can change as a function of seawater $[CO_3^{2-}]$ on monthly to seasonal timescales, although cause and effect remain elusive [*Haas et al*., 1935; *Agegian*, 1985; *Ries*, 2011b; *Williamson et al*., 2014] (Figure 2). Thus, it is important to recognize that fluctuations in some seawater carbonate system parameters, for example,

on a seasonal basis, will increase as the buffering capacity of seawater decreases with ocean acidification [*Riebesell et al*., 2009; *Melzner et al*., 2013]. Predicting the effects of ocean acidification on biomineralization in Mg-calcite organisms and higher-level effects on benthic ecosystems requires a better understanding of how these organisms produce their shells and skeletons, how seawater $\Omega_{Mg\text{-}x}$ relates to organismal fitness, a reassessment of the solubility of biogenic Mg-calcite mineral phases, and a better understanding of the controls of Mg incorporation in calcareous biominerals.

5. Conclusion

The primary conclusions of the research are as follows:

1. The $\Omega_{Cal.}$ and $\Omega_{Arag.}$ are not appropriate estimates for the saturation state of seawater with respect to Mg-calcite biominerals because they do not account for the Mg content of the calcite, which will effectively increase its solubility. Thus, species-specific $\Omega_{Mg\text{-}x}$ should be calculated from that species' actual mole % $MgCO_3$, pursuant to the equation: $\Omega_{Mg\text{-}x} = \{Mg^{2+}\}^{x}\{Ca^{2+}\}^{(1-x)}\{CO_3^{2-}\}/IAP_i$, where x is the mole fraction of Mg in substitution for Ca in the calcite lattice.
2. The Mg content for a global compilation of calcite-producing benthic marine organisms increases from pole to equator (i.e., inverse parabolic pattern from pole-to-pole).
3. The calculated $\Omega_{Mg\text{-}x}$ for a global compilation of calcite-producing benthic marine organisms with skeletons containing <5 mol % $MgCO_3$ exhibits no systematic variation with latitude, while calculated $\Omega_{Mg\text{-}x}$ for calcifiers with >5 mol % $MgCO_3$ decreases from pole to equator (i.e., parabolic pattern from pole-to-pole).
4. At present, 24% of the studied calcite-producing benthic marine organisms experience seawater undersaturation ($\Omega_{Mg\text{-}x} < 1$) worldwide, with a surprisingly higher proportion in tropical waters (~95%) versus polar waters (~5%), apparently owing to the increasing trend in Mg content of biogenic calcite from pole to equator. Most deep-sea Mg-calcite-producing organisms (>1200 m) also experience seawater undersaturation under present-day pCO_2.
5. As a result of increasing pCO_2 and decreasing $[CO_3^{2-}]$ (by up to 50% over the next 3000 years), between 34 and 57% of the surveyed marine calcifiers (including all mineralogies) across all latitudes and depths will experience seawater undersaturation.

Future work should aim to empirically constrain the stoichiometric solubilities of biogenic Mg-calcite, the controls on Mg incorporation in biogenic calcite, seasonal and spatial variability of Mg in biogenic Mg-calcite, and the vulnerability of Mg-calcite-producing organisms to future ocean acidification and warming—the latter of which can now be informed by estimates of species-specific $\Omega_{Mg\text{-}x}$ established through the present contribution.

Acknowledgments

Supporting data are included as full tables in the SI files; additional data can be obtained from M.L. (email: mlebrato13@gmail.com). Two anonymous referees are acknowledged for their valuable feedback. M.L. and M.D.I.R were supported by the "European Project on Ocean Acidification" (EPOCA), which received funding from the European Community's Seventh Framework Programme (FP7/2007-2013) under grant agreement 211384. M.L. was also supported by the Helmholtz Centre for Ocean Research Kiel (GEOMAR) and by the Center of Excellence "The Future Ocean." In addition to the images provided by the authors' institutions, images were provided by K.L. Smith of the Monterey Bay Aquarium Research Institute. A.J.A was funded by NSF grant OCE 12-55042. D.J. and H.A.R were supported by the UK Natural Environment Research Council as part of the Marine Environmental Mapping Programme (MAREMAP). M.D.L. had logistical support from Antarctica New Zealand. Additional support for work in Antarctica was provided by NSF awards ANT-0838773 to Charles D. Amsler and J.B.M.; ANT-1041022 to J.B.M., C.D.A., and Robert A. Angus. J.B.M. acknowledges the support of an endowed professorship in polar and marine biology provided by UAB. J.B.R. acknowledges support from NOAA awards NA13OAR4310186 and NA14NMF4540072 and NSF awards OCE-1459706, OCE-1437371, and MRI-1429373. W.K. and A.O. were funded by the German BIOACID program (BMBF 03F0655A). M.D.L. had support from Antarctica New Zealand and the New Zealand Antarctic Research Institute. This paper is contribution 143 from the Institute for Research on Global Climate Change at the Florida Institute of Technology and contribution 337 from the Northeastern University Marine Science Center.

References

Agegian, C. R. (1985), *The Biogeochemical Ecology of Porolithon gardineri* (Foslie), 178 pp., Honolulu, Hawaii, Uni. of Hawaii.

Andersson, A. J. (2014), The oceanic $CaCO_3$ cycle, in *Treatise on Geochemistry*, edited by H. D. Holland and K. K. Turekian, pp. 519–542, Elsevier, Oxford, U. K.

Andersson, A. J., and F. T. Mackenzie (2011), Technical comment on Kroeker et al. (2010) Meta-analysis reveals negative yet variable effects of ocean acidification on marine organisms, *Ecol. Lett.*, *14*(8), E1–E2.

Andersson, A. J., N. R. Bates, and F. T. Mackenzie (2007), Dissolution of carbonate sediments under rising pCO2 and ocean acidification: Observations from Devil's Hole, Bermuda, *Aquat. Geochem.*, *13*, 237–264.

Andersson, A. J., F. T. Mackenzie, and N. R. Bates (2008), Life on the margin: Implications of ocean acidification on Mg-calcite, high latitude and cold-water marine calcifiers, *Mar. Ecol. Prog. Ser.*, *373*, 265–273.

Aronson, R. B., S. Thatje, A. Clarke, L. S. Peck, D. B. Blake, C. D. Wilga, and B. A. Seibel (2007), Climate change and invasibility of the Antarctic benthos, *Annu. Rev. Ecol. Evol. Syst.*, *38*, 129–154.

Bischoff, W. D., F. T. Mackenzie, and F. C. Bishop (1987), Stabilities of synthetic magnesian calcites in aqueous solution: Comparison with biogenic materials, *Geochim. Cosmochim. Acta*, *51*, 1413–1442.

Borremans, C., J. Hermans, S. Baillon, L. Andre, and P. Dubois (2009), Salinity effects on the Mg/Ca and Sr/Ca in starfish skeletons and the echinoderm relevance for paleoenvironmental reconstructions, *Geology*, *37*, 351–354.

Caldeira, K., and M. E. Wickett (2003), Anthropogenic carbon and ocean pH, *Nature*, *425*, 365.

Castillo, K. D., J. B. Ries, J. F. Bruno, and I. T. Westfield (2014), The reef-building coral *Siderastrea siderea* exhibits parabolic responses to ocean acidification and warming, *Proc. R. Soc. B.*, *281*, 20141856.

Clarkson, M. O., S. A. Kasemann, R. A. Wood, T. M. Lenton, S. J. Daines, S. Richoz, F. Ohnemueller, A. Meixner, S. W. Poulton, and E. T. Tipper (2015), Ocean acidification and the Permo-Triassic mass extinction, *Science*, *348*, 329–332.

Collard, M., C. De Ridder, B. David, F. Dehairs, and P. Dubois (2015), Could the acid-base status of Antarctic sea urchins indicate a better-than-expected resilience to near-future ocean acidification?, *Global Change Biol.*, *21*, 605–617.

Comeau, S., P. J. Edmunds, N. B. Spindel, and R. C. Carpenter (2013), The responses of eight coral reef calcifiers to increasing partial pressure of CO_2 do not exhibit a tipping point, *Limnol. Oceanogr.*, *58*, 388–398.
Doney, S. C., V. J. Fabry, R. A. Feely, and J. A. Kleypas (2009), Ocean acidification: The other CO_2 problem, *Annu. Rev. Mar. Sci.*, *1*, 169–192.
Dorey, N., P. Lançon, M. Thorndyke, and S. Dupont (2013), Assessing physiological tipping point of sea urchin larvae exposed to a broad range of pH, *Global Change Biol.*, *19*, 3355–3367.
Dove, P. M., J. J. De Yoreo, and S. Weiner (2003), *Reviews in Mineralogy & Geochemistry*, *Biominer.*, vol. 54, 381 pp., Miner. Soc. of Am., Geochem. Soc, Chantilly, Va.
Dumousseaud, C., E. P. Achterberg, T. Tyrrell, A. Charalampopoulou, U. Schuster, M. Hartman, and D. J. Hydes (2010), Contrasting effects of temperature and winter mixing on the seasonal and inter-annual variability of the carbonate system in the Northeast Atlantic Ocean, *Biogeosciences*, *7*, 1481–1492.
Dupont, S., N. Dorey, M. Stumpp, F. Melzner, and M. Thorndyke (2013), Long-term and trans-life-cycle effects of exposure to ocean acidification in the green sea urchin *Strongylocentrotus droebachiensis*, *Mar. Biol.*, doi:10.1007/s00227-012-1921-x.
Eastman, J. T., M. O. Amsler, R. B. Aronson, S. Thatje, J. B. McClintock, S. C. Vos, J. W. Kaeli, H. Singh, and M. L. Mesa (2013), Photographic survey of benthos provides insights into the Antarctic fish fauna from the Marguerite Bay slope and the Amundsen Sea, *Antarct. Sci.*, *25*, 31–43.
Environmental Systems Research Institute (2011), *ArcGIS Desktop: Release 10*, Environ. Syst. Res. Inst., Redlands, Calif.
Feely, R. A., C. L. Sabine, K. Lee, W. Berelson, J. Kleypas, V. J. Fabry, and F. J. Millero (2004), Impact of anthropogenic CO_2 on the $CaCO_3$ system in the oceans, *Science*, *305*, 362–366.
Findlay, H. S., H. L. Wood, M. A. Kendall, J. I. Spicer, R. J. Twitchett, and S. Widdicombe (2011), Comparing the impact of high CO_2 on calcium carbonate structures in different marine organisms, *Mar. Biol. Res.*, *7*, 565–575.
Gage, J. D., and P. A. Tyler (1991), *Deep-Sea Biology: A Natural History of Organisms at the Deep-Sea floor*, 520 pp., Cambridge Univ. Press, Cambridge, U. K.
Guinotte, J. M., J. Orr, S. Cairns, A. Freiwald, L. Morgan, and R. George (2006), Will human induced changes in seawater chemistry alter the distribution of deep-sea scleractinian corals?, *Front. Ecol. Environ.*, *4*, 141–146.
Haas, P., G. Hill, and W. K. H. Karstens (1935), The metabolism of calcareous algae. II. The seasonal variation in certain metabolic products of *Corallina squamata* Ellis, *Ann. Bot.*, *49*, 609–619.
Hall-Spencer, J. M., R. Rodolfo-Metalpa, S. Martin, E. Ransome, M. Fine, S. M. Turner, S. J. Rowley, D. Tedesco, and M. C. Buia (2008), Volcanic carbon dioxide vents reveal ecosystem effects of ocean acidification, *Nature*, *454*, 96–99.
Holcomb, M., D. C. McCorkle, and A. L. Cohen (2010), Long-term effects of nutrient and CO_2 enrichment on the temperate coral *Astrangia poculata* (Ellis and Solander, 1786), *J. Exp. Mar. Biol. Ecol.*, *386*, 27–33.
Hönisch, B., et al. (2012), The geological record of ocean acidification, *Science*, *335*, 1058–1063.
Jokiel, P. (2011), The reef coral two compartment proton flux model: A new approach relating tissue-level physiological processes to gross corallum morphology, *J. Exp. Mar. Biol. Ecol.*, *409*, 1–12.
Jokiel, P. (2013), Coral reef calcification: Carbonate, bicarbonate and proton flux under conditions of increasing ocean acidification, *Proc. R. Soc. B.*, *280*, 20130031.
Keller, D., F. Ellias, and A. Oschlies (2014), Potential climate engineering effectiveness and side effects during a high carbon dioxide-emission scenario, *Nat. Commun.*, *5*, 3304.
Keller, D. P., A. A. Oschlies, and M. Eby (2012), A new marine ecosystem model for the University of Victoria Earth System Climate Mode, *Geosci. Model Dev.*, *5*, 1195–1220.
Key, R. M., A. Kozyr, C. L. Sabine, K. Lee, R. Wanninkhof, J. L. Bullister, R. A. Feely, F. J. Millero, C. Mordy, and T. H. Peng (2004), A global ocean carbon climatology: Results from GLODAP, *Global Biogeochem. Cycles*, *18*, GB4031, doi:10.1029/2004GB002247.
Kroeker, K. J., R. L. Kordas, R. N. Crim, and G. G. Sing (2010), Meta-analysis reveals negative yet variable effects of ocean acidification on marine organisms, *Ecol. Lett.*, *13*, 1419–1434.
Kuffner, I. B., A. J. Andersson, P. Jokiel, K. S. Rodgers, and F. T. Mackenzie (2007), Decreases in recruitment of crustose coralline algae due to ocean acidification, *Nat. Geosci.*, *1*, 114–117.
Kuffner, I. B., A. J. Andersson, P. L. Jokiel, K. S. Rodgers, and F. T. Mackenzie (2008), Decreased abundance of crustose coralline algae due to ocean acidification, *Nature Geosci.*, *1*, 114–117.
Lavigne, H., J. M. Epitalon, and J. P. Gattuso (2011), Seacarb: Seawater carbonate chemistry with R, R package version 3.0. [Available at http://CRAN.R-project.org/package=seacarb.]
Lebrato, M., and D. O. B. Jones (2009), Mass deposition event of *Pyrosoma atlanticum* carcasses off Ivory Coast (West Africa), *Limnol. Oceanogr.*, *54*, 1197–1209.
Lebrato, M., M. D. Iglesias-Rodriguez, R. A. Feely, D. Greeley, D. O. B. Jones, N. Suarez-Bosche, R. S. Lampitt, J. E. Cartes, D. R. Green, and B. Alker (2010), Global contribution of echinoderms to the marine carbon cycle: A re-assessment of the oceanic $CaCO_3$ budget and the benthic compartments, *Ecol. Monogr.*, *80*, 441–467.
Lowenstam, H. A., and S. Weiner (1989), *On Biomineralization*, Oxford Univ. Press, New York.
Mackenzie, F. T., W. D. Bischoff, F. C. Bishop, M. Loijens, J. Schoonmaker, and R. Wollast (1983), Magnesian calcites: Low temperature occurrence, solubility and solid-solution behavior, in *Carbonates: Mineralogy and Chemistry*, *Rev. in Mineral.*, edited by R. J. Reeder, pp. 97–143, Miner. Soc. of Am., Washington, D. C.
Martin, S., and J. P. Gattuso (2009), Response of Mediterranean coralline algae to ocean acidification and elevated temperature, *Global Change Biol.*, *15*, 2089–2100.
McClintock, J. B., R. A. Angus, M. R. McDonald, C. D. Amsler, S. A. Catledge, and Y. K. Vohra (2009), Rapid dissolution of shells of weakly calcified Antarctic benthic macroorganisms indicates high vulnerability to ocean acidification, *Antarct. Sci.*, *21*, 449–456.
McClintock, J. B., M. O. Amsler, R. A. Angus, R. C. Challener, J. B. Schram, C. Amsler, C. L. Mah, J. Cuce, and B. J. Baker (2011), The Mg-calcite composition of Antarctic echinoderms: Important implications for predicting the impacts of ocean acidification, *J. Geol.*, *119*, 457–466.
McCulloch, M., J. Falter, J. Trotter, and P. Montagna (2012), Coral resilience to ocean acidification and global warming through pH up-regulation, *Nat. Clim. Change*, *2*, 623–627.
McNeil, B. I., and R. J. Matear (2008), Southern Ocean acidification: A tipping point at 450-ppm atmospheric CO_2, *Proc. Natl. Acad. Sci. U.S.A.*, *105*, 18,860–18,864.
Meadows, P. S., A. Meadows, and J. M. H. Murray (2012), Biological modifiers of marine benthic seascapes: Their role as ecosystem engineers, *Geomorphology*, *157–158*, 31–48.
Melzner, F., J. Thomsen, W. Koeve, A. Oschlies, M. A. Gutowska, H. W. Bange, H. P. Hansen, and A. Körtzinger (2013), Future ocean acidification will be amplified by hypoxia in coastal habitats, *Mar. Biol.*, *8*, 1875–1888.
Milliman, J. D. (1974), *Marine Carbonate*, 375 pp., Springer, New York.

Morse, J. W., A. J. Andersson, and F. T. Mackenzie (2006), Initial responses of carbonate-rich shelf sediments to rising atmospheric pCO_2 and ocean acidification: Role of high Mg-calcites, *Geochim. Cosmochim. Acta*, *70*, 5814–5830.
Opdyke, B. N., and B. H. Wilkinson (1993), Carbonate mineral saturation state and cratonic limestone accumulation, *Am. J. Sci.*, *295*, 217–234.
Plummer, L. N., and F. T. Mackenzie (1974), Predicting mineral solubility from rate data: Application to the dissolution of Mg-calcites, *Am. J. Sci.*, *274*, 61–83.
Raz, S., S. Weiner, and L. Addadi (2000), Formation of high-magnesian calcites via an amorphous precursor phase: Possible biological implications, *Adv. Mater.*, *12*, 38–42.
Raz, S., P. C. Hamilton, F. H. Wilt, S. Weiner, and L. Addadi (2003), The transient phase of amorphous calcium carbonate in sea urchin larval spicules: The involvement of proteins and magnesium ions in its formation and stabilization, *Adv. Funct. Mater.*, *13*, 480–486.
Riebesell, U., A. Kortzinger, and A. Oschlies (2009), Sensitivities of marine carbon fluxes to ocean change, *Proc. Natl. Acad. Sci. U.S.A.*, *106*, 20,602–20,609.
Ries, J. B. (2010), Geological and experimental evidence for secular variation in seawater Mg/Ca (calcite-aragonite seas) and its effects on marine biological calcification, *Biogeosciences*, *7*, 2795–2849.
Ries, J. B. (2011a), A physicochemical framework for interpreting the biological calcification response to CO_2-induced ocean acidification, *Geochim. Cosmochim. Acta*, *75*, 4053–4064.
Ries, J. B. (2011b), Skeletal mineralogy in a high-CO_2 world, *J. Exp. Mar. Biol. Ecol.*, *403*, 54–64.
Ries, J. B., A. L. Cohen, and D. C. McCorkle (2009), Marine calcifiers exhibit mixed responses to CO_2-induced ocean acidification, *Geology*, *37*, 1131–1134.
Sewell, M. A., and G. E. Hofmann (2011), Antarctic echinoids and climate change: A major impact on the brooding forms, *Global Change Biol.*, *17*, 734–744.
Smith, K. L., H. A. Ruhl, M. Kahru, C. L. Huffard, and A. D. Sherman (2013), Deep ocean communities impacted by changing climate over 24 years in the abyssal northeast Pacific Ocean, *Proc. Natl. Acad. Sci. U.S.A.*, *110*, 19,838–19,841.
Sokolova, M. N. (1972), Trophic structure of deep-sea macrobenthos, *Mar. Biol.*, *16*, 1–12.
Steinacher, M., F. Joos, T. L. Frolicher, G. K. Plattner, and S. C. Doney (2009), Imminent ocean acidification in the Arctic projected with the NCAR global coupled carbon cycle-climate model, *Biogeosciences*, *6*, 515–533.
Tambutté, S., M. Holcomb, C. Ferrier-Pagès, S. Reynaud, E. Tambutté, D. Zoccola, and D. Allemand (2011), Coral biomineralization: From the gene to the environment, *J. Exp. Mar. Biol. Ecol.*, *408*, 58–78.
Thomsen, J., et al. (2010), Calcifying invertebrates succeed in a naturally CO_2-rich coastal habitat but are threatened by high levels of future acidification, *Biogeosciences*, *7*, 3879–3891.
Tribble, J. S., R. S. Arvidson, M. Lane, and F. T. Mackenzie (1995), Crystal chemistry and thermodynamic and kinetic properties of calcite, dolomite, apatite, and biogenic silica: Application to petrologic problems, *Sediment. Geol.*, *95*, 11–37.
Waldbusser, G. G., R. A. Steenson, and M. A. Green (2011), Oyster shell dissolution rates in estuarine waters: Effects of pH and shell legacy, *J. Shellfish Res.*, *30*, 659–669.
Walker, B. J., M. F. Miller, S. S. Bowser, D. J. Furbish, and G. A. R. Gualda (2013), Dissolution of ophiuroids ossicles on the shallow Antarctic shelf: Implications for the fossil record and ocean acidification, *Palaios*, *28*, 317–332.
Watson, S. A., L. S. Peck, P. A. Tyler, P. C. Southgate, K. S. Tan, R. W. Day, and S. A. Morley (2012), Marine invertebrate skeleton size varies with latitude, temperature and carbonate saturation: Implications for global change and ocean acidification, *Global Change Biol.*, *18*, 3026–3038.
Williamson, C. J., J. Najorka, R. Perkins, M. L. Yallop, and J. Brodie (2014), Skeletal mineralogy of geniculate corallines: Providing context for climate change and ocean acidification research, *Mar. Ecol. Prog. Ser.*, *513*, 71–84.
Wood, H. L., J. I. Spicer, and S. Widdicombe (2008), Ocean acidification may increase calcification rates, but at a cost, *Proc. R. Soc. B.*, *275*, 1767–1773.
Yamamoto-Kawai, M., F. A. McLaughlin, E. C. Carmack, S. Nishino, and K. Shimada (2009), Aragonite undersaturation in the Arctic Ocean: Effects of ocean acidification and sea ice melt, *Science*, *326*, 1098–1100.
Zeebe, R. E. (2012), History of seawater carbonate chemistry, atmospheric CO_2, and ocean acidification, *Annu. Rev. Earth Planet. Sci.*, *40*, 141–165.
Zoccola, D., et al. (2015), Bicarbonate transporters in corals point towards a key step in the evolution of cnidarian calcification, *Sci. Rep.*, *5*, 09983.